Research Article | Vol. 27, No. 10 | 13 May 2019 | OPTICS EXPRESS 14030
Optics EXPRESS

Long cavity ring fiber mode-locked laser with decreased net value of nonlinear polarization rotation

L. A. Rodriguez-Morales,[1] I. Armas-Rivera,[1] B. Ibarra-Escamilla,[1] O. Pottiez,[2] H. Santiago-Hernandez,[3] M. Durán-Sánchez,[1,4] M. V. Andrés,[5] and E. A. Kuzin[1,*]

[1]*Instituto Nacional de Astrofísica, Óptica y Electrónica (INAOE), L. E. Erro 1, Sta. Ma. Tonantzintla, Pue. 72824, Mexico*
[2]*Centro de Investigaciones en Óptica (CIO), Loma del Bosque 115, Col. Lomas del Campestre, León, Gto. 37150, Mexico*
[3]*Universidad de Guadalajara, Departamento de Electrónica, Av. Revolución 1500, Guadalajara, Jalisco, 44840, Mexico*
[4]*CONACYT-Instituto Nacional de Astrofísica, Óptica y Electrónica, A. P. 51 y 216, CP 72000, Puebla, Pue., Mexico*
[5]*Departamento de Física Aplicada y Electromagnetismo, ICMUV, Universidad de Valencia, C/Dr. Moliner, 50, 46100 Burjassot, Spain*
[*]*ekuz@inaoep.mx*

Abstract: We investigate a new configuration of a mode-locked fiber laser by using a nonlinear polarization rotation-based design to generate soliton pulses with low repetition rate. Unlike with previously reported configurations, we introduce a Faraday mirror after the first half of the cavity length to counteract the nonlinear polarization rotation effects. The total cavity length is 437 m including a 400-m long twisted SMF-28 fiber. The fiber was twisted to cancel the linear birefringence and to ensure that the polarization ellipticity is not altered as the pulse travels along the fiber. The strict control of polarization yields a stable relation between the polarization state of the pulses propagating in the cavity and the regimes of generation. Depending on the polarization state we observed three different emission regimes, the single soliton regime (SR), conventional noise-like pulses (NLP) and noise-like square-waveform pulse (NLSWP). In the SR, a 467.2 kHz train of solitons was obtained with pulse duration of 2.9 ps at 1558.7 nm.

1. Introduction

Ultrafast lasers have attracted significant interest due to their potential for applications like surgery [1], high-precision micromachining [2] and multiphoton microscopy (MPM) [3]. In the last case the fiber soliton sources can be especially useful because of their capacity of generating ultrashort pulses in the wavelength range from 1530 nm to 2000 nm using Er, Tm, Ho doped fibers and the effect of soliton self-frequency shift [4]. A high-repetition train of ultrashort pulses causes the effect of thermal accumulation [5,6] which can be beneficial in some cases, however it is undesirable for applications such as MPM. The repetition rate can be reduced by using pulse pickers such as Pockels cells or acousto-optic modulators, however this method is energetically inefficient and increases the complexity of the setup. Because the repetition rate of a mode-locked laser is inversely proportional to its resonator length, the repetition rate can be reduced simply by lengthening the cavity. In contrast to solid-state lasers, which require critical alignment, fiber lasers are more prone to achieve lower repetition rates with the convenience and simplicity of elongating a fiber cavity.

The long cavity lasers were studied mainly with the purpose to increase the pulse energy in the configurations with net-normal dispersion. For example, Kobtsev et al. [7]

#361168 https://doi.org/10.1364/OE.27.014030
Journal © 2019 Received 6 Mar 2019; revised 10 Apr 2019; accepted 16 Apr 2019; published 30 Apr 2019

Optics EXPRESS

demonstrated the generation of pulses with repetition rate of 77 kHz and pulse energy of 3.9 μJ using the nonlinear polarization rotation (NPR) for mode-locking in ytterbium-doped fiber (YDF) fiber laser. However, the pulse duration was 3 ns. The generation of pulses with the repetition rate of 35.1 kHz and pulse energy of 1.7 μJ was demonstrated in [8] using NPR for mode-locking in an Er-doped fiber laser. To have net normal cavity dispersion, 2.3 km of nonzero dispersion shifted fiber and 1.25 km of dispersion compensating fiber were used. The pulse duration was 13 ns. Different techniques for mode locking in low repetition rate lasers were used. A low repetition rate laser using SESAM for mode locking was demonstrated in [9]. For different cavity lengths, wave-breaking-free pulse with 2.9 nJ - 6.9 nJ pulse energy and 870 kHz - 187 kHz repetition rate has been achieved. In [10] a nonlinear amplifier loop mirror (NALM) was used for mode-locking. In this laser, pulses with an energy of 12.4 μJ at a repetition rate of 41.7 kHz were generated. The pulse duration was 4.3 ns.

It was shown that long cavity lasers with normal dispersion can generate pulses with giant linear chirp, giant chirp oscillators (GCO), so that the pulses can be externally compressed to produce ultrashort pulses with high energy [11]. In this work. pulse compression from 150 ps to 670 fs was demonstrated. The repetition rate was 3 MHz. Using this technique several works followed. For example, in [12] a passively mode-locked YDF laser with a repetition rate of 1.8 MHz was reported. The laser was hybridly mode-locked via nonlinear polarization evolution and a semiconductor saturable absorber mirror. It generated chirped 3.8 ps long pulses with a pulse energy of 1.0 nJ, which could be dechirped to a pulse duration of 93 fs. One drawback of fiber lasers is their dependence on the environmental conditions. In [13] an environmentally stable GCO operating at 1030 nm using all-PM cavity and a NALM as the mode locker was demonstrated. Pulses with energy of 10 nJ and duration of 68 ps at a repetition rate of 1.7 MHz were generated. Externally, the pulses were compressed down to 370 fs. The technique using nonlinear polarization evolution in a PM fiber and a Faraday Mirror (FM) to decrease the influence of environmental conditions was used in [14]. The generation of 17.8 ps pulses at 948 kHz repetition rate was obtained. The bandwidth was about 2.2 nm, which indicates that pulses can be compressed, however it was not demonstrated in the paper. All the above mentioned lasers used YDF as the active medium, which is most appropriate for this technique.

Lasers with anomalous dispersion cavities can generate fundamental solitons due to the balancing between dispersion and Kerr nonlinearity. However, the generation of solitons with low repetition rate in this regime is a quite challenging task. Instead of a single soliton in the cavity, these lasers tend to generate multiple solitons, molecules of solitons, noise like pulses etc. The dynamics of the generation is quite complicated and is the subject of many research activities, see for example [15] and references therein. The sensitivity to environmental perturbations is another challenge. In [16] was demonstrated a laser with < 0.04% amplitude fluctuation with the use of carbon nanotubes for mode locking.

There are only few reports on long cavity soliton lasers. The generation of solitons with sub-MHz repetition rate was demonstrated in [17]. The generation of solitons from a 720-m long cavity was demonstrated in [18], however, multiple solitons were present in the cavity and the repetition rate was high, at least higher than 10 MHz (no precise data were provided in the paper). One of the reasons of the difficulties of the generation of low-frequency trains of solitons from long cavity lasers arises from their high nonlinearity and large dispersion [19].

One of the commonly used technique for mode-locking is based on NPR. In these configurations, the polarization rotates from an azimuth corresponding to low transmission through the polarizer at low pulse power to an azimuth corresponding to high transmission for high-power pulses. In long cavities the NPR can be easily overdriven. It means that when the polarization rotation is larger than a certain critical value, the transmission degrades with a further increase of the cavity length or power, thereby preventing the generation of solitons with low repetition rate. Some experiments show that stable operation can be reached for a

Optics EXPRESS

cavity fiber length shorter that three soliton periods [20]. For long cavity lasers made from low-birefringence fibers another problem arises from residual birefringence, which depends on environmental conditions. Residual birefringence results in uncontrollable polarization variations in the cavity. However, polarization plays a critical role in many laser configurations; for example, in a ring laser configuration based on NPR. The NPR rate depends on the ellipticity of the propagating pulses and therefore can be affected strongly by residual birefringence. The effect of residual birefringence may be especially important for long cavity lasers.

Recently, we demonstrated stable and predictable switching between different regimes of generation in a mode-locked fiber ring laser where fiber twist was used to cancel residual birefringence [21]. In the present work we propose and investigate a method to realize the cancellation of excessive NPR in a long mode-locked fiber ring laser. We introduce a circulator and a FM in the middle of the cavity so that after propagation through half the cavity the elliptical polarization changes handedness and therefore the handedness of the NPR in the second half of the cavity is opposed to that in the first half. The results are a quite low net NPR in the long cavity. We used twisted fiber in the cavity to maintain constant the ellipticity of polarization, which allowed a strict control of the polarization state. The strict control of polarization gave us a stable relation between the polarization state of the pulses propagating in the cavity and the regimes of generation. We found three different emission regimes in our configuration by changing the initial polarization conditions: the soliton regime (SR), conventional nose-like pulses (NLP), and squared-waveform noise-like pulses (NLSWP). The total length of the cavity is 437 m. In the SR we obtained a 467.2 kHz train of 2.9-ps pulses. To the best of our knowledge it is the lowest repetition rate train of solitons ever reported.

2. Experimental setup

Figure 1 shows the experimental setup. The ring cavity includes a double-pass amplifier (dashed box) and two pieces of 200-m long twisted SMF-28 fiber. The fibers were twisted with a twist rate of 7 turns/m and wounded on a 50-cm diameter cylinder. Previously we used the same technique for the design of a nonlinear optical loop mirror (NOLM), see [22] where the details of the twisted fiber characterization can be found. A 50/50 coupler, a polarizer, and an in-line polarization controller (PC1, model PLC-900-Thorlabs) close the ring cavity. The PC1 allows the adjustment of the polarization ellipticity by the pressure applied to the fiber and independently allows adjusting the azimuth by rotation. The double-pass amplifier is made up of an optical circulator (C1), a 45-cm long erbium-doped fiber (EDF) with an absorption coefficient of 80 dB/m at 1530 nm, and a Faraday mirror (FM1). The FM1 allows compensation of the EDF birefringence so that the polarization at the circulator output is orthogonal to the polarization at its input. It is especially important for the erbium-doped fiber amplifier (EDFA) because EDF birefringence may depend on temperature and pump power. A 980-nm laser diode, used as pump source, was coupled to the EDF through a wavelength division multiplexer (WDM). The handedness of NPR in Fiber 1 depends on the handedness of the elliptical polarization (right or left) at the EDFA output. After Fiber 1, the pulses pass through the circulator from port 1 to port 2 without change of the polarization ellipticity. The second Faraday mirror (FM2) inserted between Fiber 1 and Fiber 2 changes the handedness of ellipticity, and then the reflected pulses pass from port 2 to port 3 without change of the polarization ellipticity. So, the pulses propagate in Fiber 2 with handedness of ellipticity opposite to that in Fiber 1. Therefore, NPR in Fiber 2 can compensate NPR in Fiber 1 and annihilate any possible excess of NPR.

Optics EXPRESS

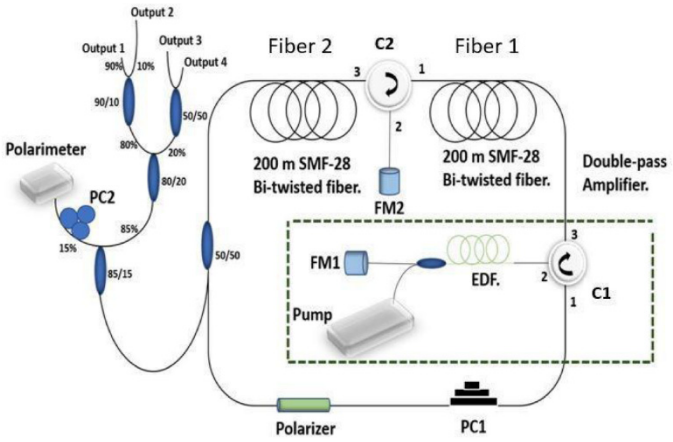

Fig. 1. Schematic diagram of the passively mode-locked EDFL.

Note that the use of the FM in [14] has a completely different purpose as compared with our work. In that work FM was used to cancel the environmentally dependent linear phase shift in PM fiber and so to achieve stable operation. In contrast, in the present work we use FM to compensate NPR by changing the handedness of polarization ellipticity. It should be mentioned that the handedness of the polarization ellipticity can be changed by reflection from a conventional mirror as well.

In the fibers without linear birefringence it is convenient to consider NPR in the basis of circularly polarized components. In this basis the Kerr effect causes a phase shift between circularly polarized components without energy exchange between them. Therefore, the polarization ellipticity is not altered during propagation and the phase shift only causes a rotation of the polarization ellipse. The angle of NPR is equal to $-\frac{1}{3}\gamma P A_c L$, where γ is nonlinearity, P - power, L - fiber length, and A_c is the third Stokes parameter equal to difference between powers of left and right circularly polarized components. The details can be found in [23]. We calculate NPR and transmission through the polarizer for a fiber length of 400 m and nonlinearity of 1.5 $(\text{W-km})^{-1}$ for two cases: without change of handedness during propagation and with a change at half of the length. Figure 2 shows the result when ellipticity is 10^0. The attenuation caused by the circulator and FM was taken as 10%.

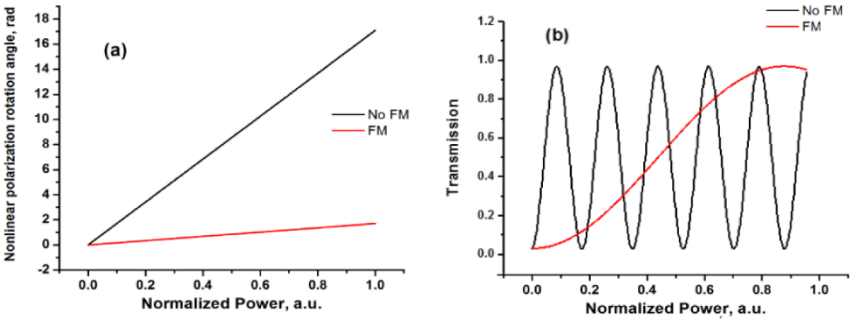

Fig. 2. a) NPR angle, with a FM at half length (red line), with no FM (black line). b) Transmission through the polarizer considering the minimal transmission at low power, with FM at half length (red line), and no FM (black line).

We can see that total NPR is approximately ten times less in our configuration compared with conventional lasers using NPR for mode-locking.

Optics EXPRESS

The dispersion of the 400-m SMF-28 fiber is 7.5 ps/nm. The cavity also includes 2 m of OFS-980 fiber (the WDM ports), which contributes with a dispersion of –0.013 ps/nm for the double pass in the amplifier section, 0.45-m of EDF with dispersion of 0.006 ps/nm for the double pass, and 0.4-m PM panda fiber at the polarizer output with dispersion of approximately 0.001 ps/nm. The total cavity length is 437 m with net anomalous dispersion of approximately 7.6 ps/nm. The output port of the 50/50 coupler is spliced with an 85/15 coupler. The 15% port is used to monitor the polarization state inside the cavity using a polarimeter (PAX5710R3-T, Thorlabs). Generally, the polarization at the 50/50 coupler input is not the same as at the polarimeter input due to some residual birefringence of the fibers and couplers. Nevertheless, this birefringence is compensated by a polarization controller (PC2) included before the polarimeter input. To adjust PC2 we measured the polarization ellipticity at the output of the 50/50 coupler and then adjusted PC2 to have the same polarization ellipticity at the output of PC2. The signal at the 85% port of the 85/15 coupler is further split using three additional couplers, in order to produce outputs 1 to 4. The pulse duration was measured with an autocorrelator (FR-103XL) at Output 1, the optical spectrum was measured at Output 2, the output pulses were detected by a 10-GHz photodetector with a 20-GHz sampling oscilloscope at Output 3, whereas Output 4 was used for triggering the sampling oscilloscope.

3. Results and discussions

To begin we started the laser generation in continuous wave mode, rotated PC1 and measured by the polarimeter the azimuths corresponding to minimal and maximal output powers. These azimuths correspond to minimal and maximal transmission through the polarizer. In the following text the minimal transmission angle is referred to as 0° and the angle of maximal transmission is 90°. When the mode-locked operation starts, the azimuth rotates from the initial angle established by PC1 towards angles corresponding to higher transmission through the polarizer. This rotation was measured by the polarimeter. After this rotation the final azimuth may reach or not the angle of maximal transmission.

Experimentally we found that the regimes of mode-locking operation depend on the initial azimuth and ellipticity. At different values of initial azimuth and ellipticity we set the pump power at 285 mW and applied a mechanical stimulation to the fiber to start mode-locking operation. Depending of the initial conditions the operation was started in different regimes. The results are shown in Fig. 3. The red circles in Fig. 3 show the region in which mode locking operation is started in NLSWP regime, the black circles show the region with NLP regime, whereas the blue circles correspond to the SR. Outside these regions the mode-locking operation was not found. Below we consider in detail these three regimes.

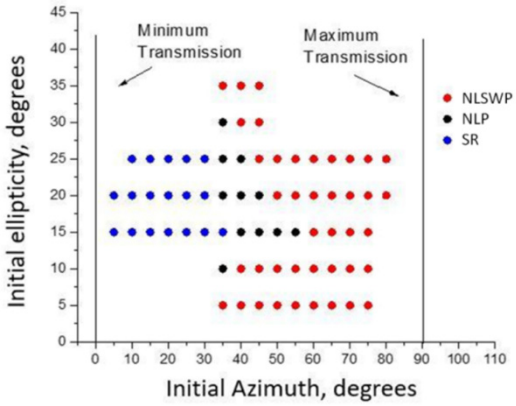

Fig. 3. Summary of the generation modes obtained in the laser; red circles – NLSWPs, black circles - NLPs, blue circles – solitons.

Optics EXPRESS

3.1. Soliton regime (SR)

At the polarization states marked by blue circles in Fig. 3 the laser started to generate pulses whose spectrum presented Kelly sidebands, which are typical for soliton generation. Figure 4 shows the characteristics obtained at the initial azimuth of 30°, ellipticity of 15°, and pump power of 285 mW. The cavity is filled with pulses. The measurement setup does not allow measuring individually closely spaced pulses; however, we can see that at least two of the highest peaks are repeated with a periodicity corresponding to the roundtrip time of 2.140 μs. This allows assuming that the laser generates a periodic train of pulses at least over several round trips. The spectrum, shown in Fig. 4(b), presents Kelly sidebands, the typical signature of solitons [24]. The spectrum has a maximum at 1558.7 nm, the dashed line shows a fit by the spectrum of a $sech^2$ pulse with FWHM of 1.12 nm. The comparison between the fitting curve and the measured spectrum suggests some red shift of the soliton spectra, which indicates that the laser emission consists of solitons with different durations, the shortest ones being red shifted by soliton self-frequency shift. As a result of the red shift of a fraction of the solitons, the average spectrum shown in Fig. 4(b) is asymmetric, skewed to longer wavelengths. The autocorrelation trace shows a double-scaled structure typical of NLP. Usually the origin of the pedestal is attributed to the chaotic, nonstationary dynamics of solitons confined within the cavity [25].

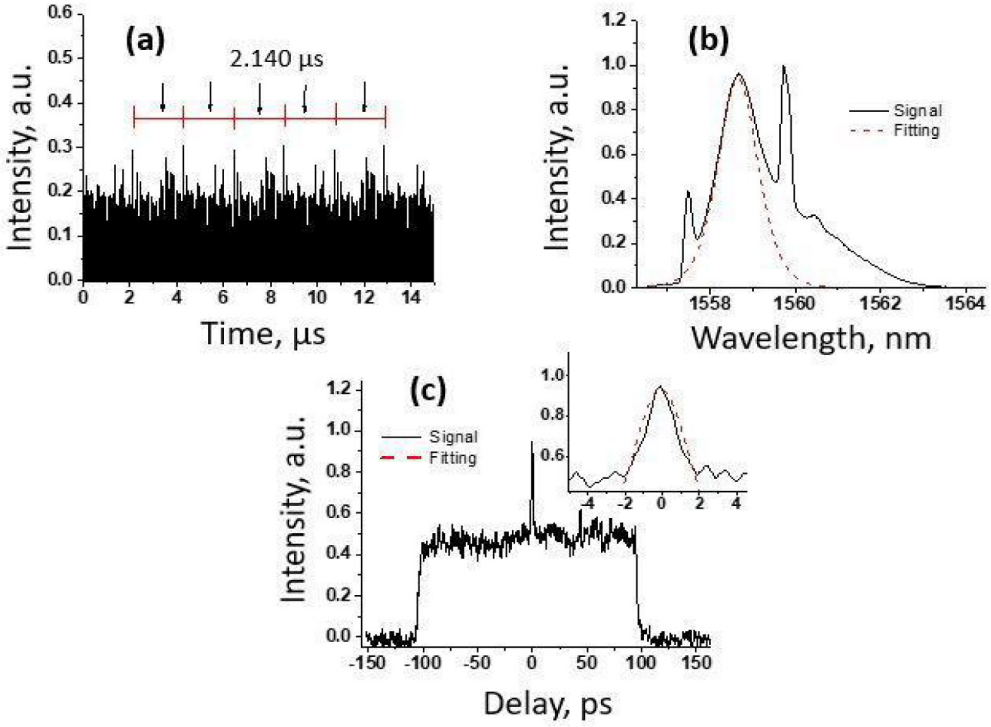

Fig. 4. Solitonic regime at pump power of 285 mW. (a) The temporal profile, (b) the output spectrum, and (c) the autocorrelation trace.

The decrease of pump power causes a transition to a regime of more widely spaced solitons, see Fig. 5(a) which shows the waveform at a pump power of 100 mW. As presented in Fig. 5(b), the central wavelength of the optical spectrum is 1558.77 nm with 1.4 nm 3-dB bandwidth. The red shift is still present; however, it is much less significant that in the previous case. When the number of pulses is less than some critical value, the solitons are separated [26], this phenomenon causes the decrease of the pedestal of the autocorrelation

Optics EXPRESS

trace, see Fig. 5(c). Slight asymmetry of the autocorrelation trace was caused by slight shift of the micrometer screw which changes the length of one hand of the autocorrelator.

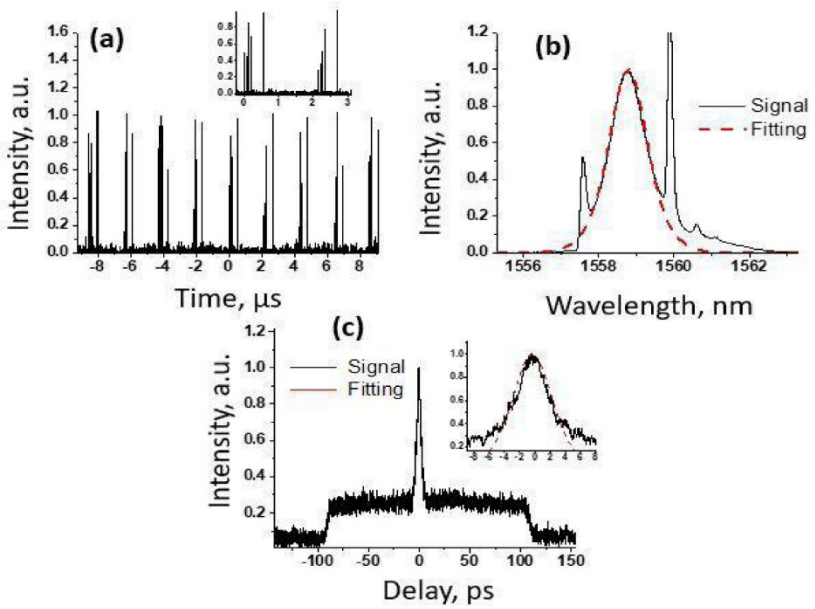

Fig. 5. Solitonic regime at pump power of 100 mW. (a) The temporal profile, (b) the output spectrum, and (c) the autocorrelation trace.

The single soliton generation is achieved at pump powers from 76 mW to 66 mW. Figure 6(a) shows a pulse train with a period of 2.140 μs, corresponding to a repetition rate of 467.2 kHz. At 70 mW pump power, the average output power is ~24 μW and the estimated peak power is ~ 17.7 W with an energy of 51.3 pJ. The inset shows a close-up on a single peak measured with a 2-GHz bandwidth oscilloscope. The spectrum, shown in Fig. 6(b), is centered on 1558.7 nm and has a 3-dB bandwidth of 1.1 nm.

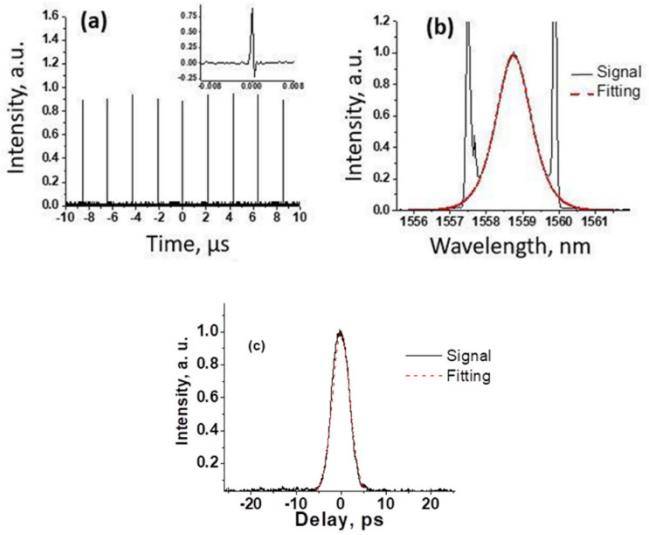

Fig. 6. Single pulse in the cavity soliton generation; (a) temporal profile, (b) the output spectrum, and (c) the autocorrelation trace.

Optics EXPRESS

Figure 6(c) illustrates the pedestal-free autocorrelation trace, which is well fitted by the corresponding autocorrelation trace for a $sech^2$ temporal profile. The FWHM of the autocorrelation trace is measured to be 4.6 ps, resulting in a pulse duration of 2.9 ps. From the measurements shown in Fig. 6(b) and (c), we calculate the time-bandwith product of 0.358 which shows that the pulse is nearly transform limited. The autocorrelation trace shows an isolated peak in the entire autocorrelation window (around 200 ps) without any small secondary peaks. The spectrum does not reveal any modulation which is characteristic for stable packets of soliton like soliton molecules. Therefore, in spite that there is some gap between the autocorrelator window and the oscilloscope response time, all these data give the evidence that a single pulse presents in the cavity.

If the pump power decreases, the mode-locked operation disappears, on the other hand when the pump power is increased, the aforementioned behavior in Fig. 5 return.

3.2. Noise-like square-waveform pulses

Figure 7 shows the characteristics of NLSWPs measured at different pump powers. The azimuth was set at 60° and the ellipticity at 25°. All spectra, Fig. 7(a), are centered at 1563 nm and have a 3-dB bandwidth of 6.1 nm, much larger than in the case of the SR. The spectra are fit well with a $sech^2$ shape and do not show appreciable shape or bandwidth changes as the pump power changes. Figure 7(b) shows the pulse train with a repetition rate of 467.2 kHz, which corresponds to fundamental mode-locking for a cavity length of 437 m. Figure 7(c) shows pulse waveforms at different pump powers. The pulses have a quasi-rectangular profile with roughly constant intensity and a duration that increases with pump power. The maximum pulse duration was about 26 ns. The behavior of the spectra and the waveforms is similar to that observed for the dissipative soliton resonance regime (DSR) [27,28]. However, the autocorrelation trace, Fig. 7(d), shows a double structure with a short peak riding long pedestal, which is typical of NLPs. The characteristics of the square pulses reported in this work are similar to those reported before by other authors [29,30].

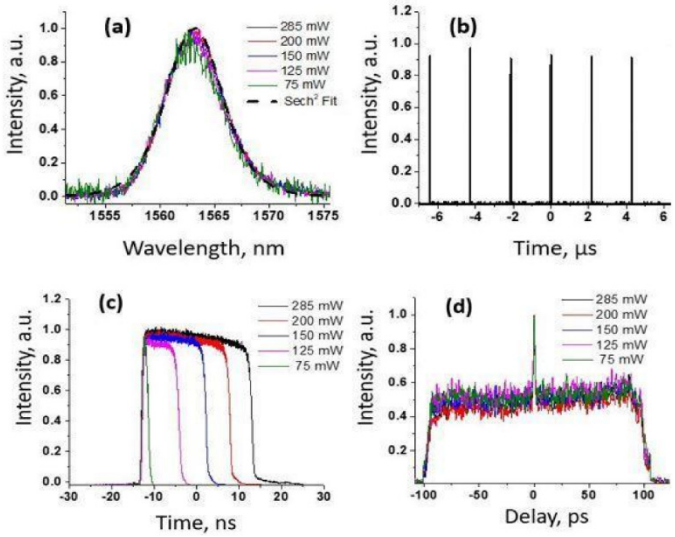

Fig. 7. Noise-like squared waveform pulses; (a) optical spectra for different pump powers, (b) train of pulses with fundamental repetition rate of 467.2 kHz, (c) waveforms at different pump powers, (d) autocorrelation traces.

Finally, Fig. 8 shows the energy per pulse and the 3-dB pulse duration at different pump powers.

Optics EXPRESS

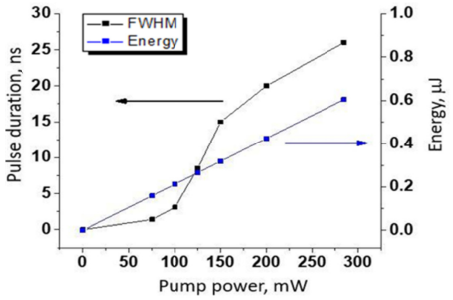

Fig. 8. Dependence of pulse duration (black line) and pulse energy (blue line) on pump power.

3.3. NLP regime

When we adjust the polarization to the states shown by black circles in Fig. 2 the NLSWP regime switches to the generation of NLPs. Figure 9(a) shows the oscilloscope traces at 285 mW pump power; the azimuth is set to 60° and the ellipticity to 15°. The black line shows the trace obtained in single-shot mode of the sampling oscilloscope, whereas the red line shows the average trace. Because of the use of a sampling oscilloscope, the single shot traces do not show exactly one single pulse. Despite this, the comparison between single-shot traces and averaged traces makes it possible to conclude that the pulses consist of a large number of separated pulses which are moving randomly within their envelope, similarly to what was observed in [31].

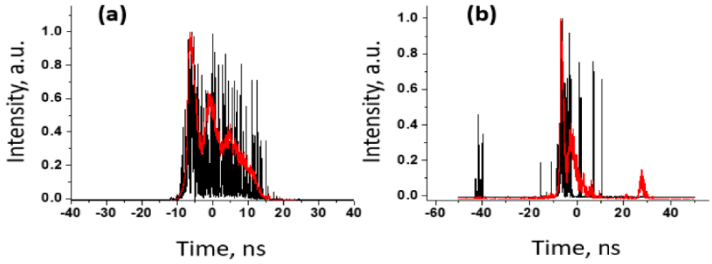

Fig. 9. Waveforms of NLPs at 285 mW pump power (a) and 125 mW pump power (b). Black lines show single-shot oscilloscope traces; red lines show averaged oscilloscope traces.

When the pump power decreases for the same initial polarization conditions, the duration of the envelope decreases, as we can see in Fig. 9(b) where the pump power is set to 125 mW. Besides, we can see in Fig. 9(b) that the packet breaks into several pulses. Figure 10(a) shows the typical NLP double-scaled autocorrelation traces both for 285 mW and 125 mW pump power values. The ratio between pedestal and peak is less than 0.5 and tends to be smaller for lower pump powers. The FWHM of the narrow peak is about 2.9 ps in both cases. The optical spectra for both pump powers are shown in Fig. 10(b). We observed some red shift, which is probably caused by Raman self-frequency shift.

Optics EXPRESS

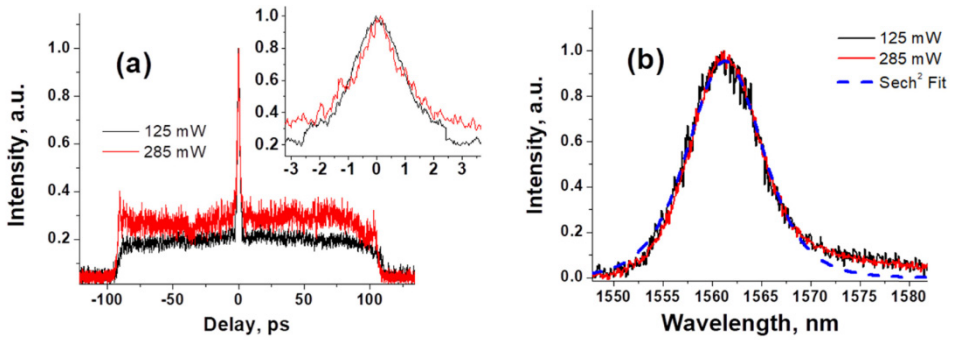

Fig. 10. Autocorrelation traces (a) and spectra (b) of NLPs for two different pump powers: black lines - 125 mW, red lines - 285 mW. Inset shows close-up on central peak of autocorrelation traces.

4. Conclusions

In conclusion, we present a fiber ring laser with decreased net nonlinear polarization rotation and strict control of the polarization state in the cavity. The strict control makes it possible to investigate how the generation mode depends on the polarization state. We observed three different emission regimes at three well defined areas of the polarization state, namely NLSWP, NLP and SR. The laser is able to generate 2.9 ps solitons with a repetition rate of 467.2 kHz. Such ultra-low repetition rate as well as short pulse width makes this mode-locked all-fiber laser a suitable oscillator to directly seed a fiber amplifier, which can be used as a compact source for high-power applications, micromachining, biomedical diagnostics and lidar systems.

Funding

Consejo Nacional de Ciencia y Tecnología, project 287315.

Acknowledgments

I. Armas-Rivera thanks Consejo Nacional de Ciencia y Tecnología postdoctoral fellow 28667.

References

1. T. Juhasz, F. H. Loesel, R. M. Kurtz, Ch. Horvath, J. F. Bille, and G. Mourou, "Corneal Refractive Surgery with Femtosecond Lasers," IEEE J. Sel. Top. Quantum Electron. **5**(4), 902–910 (1999).
2. B. W. Liu, M. L. Hu, X. H. Fang, Y. Z. Wu, Y. J. Song, L. Chai, C. Y. Wang, and A. M. Zheltikov, "High-power wavelength-tunable photonic-crystal-fiber-based oscillator-amplifier-frequency-shifter femtosecond laser system and its applications for material microprocessing," Laser Phys. Lett. **6**(1), 44–48 (2009).
3. W. Denk, J. H. Strickler, and W. W. Webb, "Two-photon laser scanning fluorescence microscopy," Science **248**(4951), 73–76 (1990).
4. K. Wang, N. G. Horton, K. Charan, and C. Xu, "Advanced Fiber Soliton Sources for Nonlinear Deep Tissue Imaging in Biophotonics," IEEE J. Sel. Top. Quantum Electron. **20**(2), 50–60 (2014).
5. S. M. Eaton, H. Zhang, M. L. Ng, J. Li, W. J. Chen, S. Ho, and P. R. Herman, "Transition from thermal diffusion to heat accumulation in high repetition rate femtosecond laser writing of buried optical waveguides," Opt. Express **16**(13), 9443–9458 (2008).
6. S. Juodkazis, H. Misawa, and I. Maksimov, "Thermal accumulation effect in three-dimensional recording by picosecond pulses," Appl. Phys. Lett. **85**(22), 5239–5241 (2004).
7. S. Kobtsev, S. Kukarin, and Y. Fedotov, "Ultra-low repetition rate mode-locked fiber laser with high-energy pulses," Opt. Express **16**(26), 21936–21941 (2008).
8. B. Nyushkov, V. Denisov, S. Kobtsev, V. Pivtsov, N. Kolyada, A. Ivanenko, and S. Turitsyn, "Generation of 1.7-μJ pulses at 1.55 μm by a self-mode locked all-fiber laser with a kilometers-long linear-ring cavity," Laser Phys. Lett. **7**(9), 661–665 (2010).
9. X. Tian, M. Tang, X. Cheng, P. P. Shum, Y. Gong, and C. Lin, "High-energy wave-breaking-free pulse from all-fiber mode-locked laser system," Opt. Express **17**(9), 7222–7227 (2009).

Optics EXPRESS

10. A. Ivanenko, S. Kobtsev, S. Smirnov, and A. Kemmer, "Mode-locked long fibre master oscillator with intra-cavity power management and pulse energy > 12 μJ," Opt. Express **24**(6), 6650–6655 (2016).
11. W. H. Renninger, A. Chong, and F. W. Wise, "Giant-chirp oscillators for short-pulse fiber amplifiers," Opt. Lett. **33**(24), 3025–3027 (2008).
12. H. Sayinc, D. Mortag, D. Wandt, J. Neumann, and D. Kracht, "Sub-100 fs pulses from a low repetition rate Yb-doped fiber laser," Opt. Express **17**(7), 5731–5735 (2009).
13. M. Erkintalo, C. Aguergaray, A. Runge, and N. G. R. Broderick, "Environmentally stable all-PM all-fiber giant chirp oscillator," Opt. Express **20**(20), 22669–22674 (2012).
14. S. Boivinet, J.-B. Lecourt, Y. Hernandez, A. A. Fotiadi, M. Wuilpart, and P. Mégret, "All-Fiber 1-μm PM Mode-Lock Laser Delivering Picosecond Pulses at Sub-MHz Repetition Rate," IEEE Photonics Technol. Lett. **26**(22), 2256–2259 (2014).
15. X. Liu and Y. Cui, "Revealing the behavior of soliton buildup in a mode-locked laser," Advanced Photonics **1**(1), 1 (2019).
16. X. Liu, D. Han, Z. Sun, C. Zeng, H. Lu, D. Mao, Y. Cui, and F. Wang, "Versatile multi-wavelength ultrafast fiber laser mode-locked by carbon nanotubes," Sci. Rep. **3**(1), 2718 (2013).
17. C. Cuadrado-Laborde, J. L. Cruz, A. Díez, and M. V. Andrés, "Sub-picosecond ultra-low frequency passively mode-locked fiber laser," Appl. Phys. B **122**(11), 273 (2016).
18. X. Liu, "Coexistence of strong and weak pulses in a fiber laser with largely anomalous dispersion," Opt. Express **19**(7), 5874–5887 (2011).
19. R. I. Woodward, "Dispersion engineering of mode-locked fibre lasers," J. Opt. **20**(3), 033002 (2018).
20. K. Tamura, C. R. Doerr, H. A. Haus, and E. P. Ippen, "Soliton fiber ring laser stabilization and tuning with a broad intracavity filter," IEEE Photonic Tech. L. **6**(6), 697–699 (1994).
21. H. Santiago-Hernández, Y. E. Bracamontes-Rodríguez, G. Beltrán-Pérez, I. Armas-Rivera, L. A. Rodríguez-Morales, O. Pottiez, B. Ibarra-Escamilla, M. Durán-Sánchez, M. V. Hernández-Arriaga, and E. A. Kuzin, "Initial conditions for dissipative solitons in a strict polarization-controlled passively mode-locked Er-Fiber laser," Opt. Express **25**(21), 25036–25045 (2017).
22. L. A. Rodríguez-Morales, I. Armas-Rivera, M. Avazpour, G. Beltran-Pérez, H. Santiago-Hernandez, B. Ibarra-Escamilla, M. Durán-Sánchez, O. Pottiez, and E. A. Kuzin, "Experimental investigation of polarization imbalanced nonlinear loop mirror with double-sense twisted fiber as a filter to clean up solitons," J. Opt. **20**(1), 015502 (2018).
23. S. F. Feldman, D. A. Weinberger, and H. G. Winful, "Polarization instability in a twisted birefringent optical fiber," J. Opt. Soc. Am. B **10**(7), 1191–1201 (1993).
24. S. M. Kelly, "Characteristic sideband instability of periodically amplified average soliton," Electron. Lett. **28**(8), 806 (1992).
25. C. Lecaplain, P. Grelu, J. M. Soto-Crespo, and N. Akhmediev, "Dissipative rogue waves generated by chaotic pulse bunching in a mode-locked laser," Phys. Rev. Lett. **108**(23), 233901 (2012).
26. D. Korobko, R. Gumenyuk, I. Zolotovskii, and O. Okhotnikov, "Multisoliton complexes in fiber lasers," Opt. Fiber Technol. **20**(6), 593–609 (2014).
27. I. Armas-Rivera, C. Cuadrado-Laborde, A. Carrascosa, E. A. Kuzin, G. Beltrán-Pérez, A. Díez, and M. V. Andrés, "Dissipative soliton resonance in a full polarization-maintaining fiber ring laser at different values of dispersion," Opt. Express **24**(9), 9966–9974 (2016).
28. Z. C. Luo, W. J. Cao, Z. B. Lin, Z. R. Cai, A. P. Luo, and W. C. Xu, "Pulse dynamics of dissipative soliton resonance with large duration-tuning range in a fiber ring laser," Opt. Lett. **37**(22), 4777–4779 (2012).
29. H. Liu, X. W. Zheng, N. Zhao, Q. Y. Ning, M. Liu, Zh. Ch. Luo, A. P. Luo, and W. Ch. Xu, "Generation of Multiwavelength Noise-Like Square-Pulses in a Fiber Laser," IEEE Photonics Technol. Lett. **26**(19), 1990–1993 (2014).
30. J. Liu, Y. Chen, P. Tang, C. Xu, C. Zhao, H. Zhang, and S. Wen, "Generation and evolution of mode-locked noise-like square-wave pulses in a large-anomalous-dispersion Er-doped ring fiber laser," Opt. Express **23**(5), 6418–6427 (2015).
31. Y. Jeong, L. A. Vazquez-Zuniga, S. Lee, and Y. Kwon, "On the formation of noise-like pulses in fiber ring cavity configurations," Opt. Fiber Technol. **20**(6), 575–592 (2014).